New Perspectives on Droop Control in AC Microgrid

Yao Sun, Xiaochao Hou, Jian Yang, Hua Han, Mei Su, and Josep M. Guerrero

***Abstract*—Virtual impedance, angle droop, and frequency droop control play important roles in maintaining system stability, and load sharing among distributed generators (DGs) in microgrid. These approaches have been developed into three totally independent concepts, but a strong correlation exists. In this letter, their similarities and differences are revealed. Some new findings are established as follows: 1) the angle droop control is intrinsically a virtual inductance method; 2) virtual inductance method can also be regarded as a special frequency droop control with a power derivative feedback; and 3) the combination of virtual inductance method and frequency droop control is equivalent to the proportional–derivative type frequency droop, which is introduced to enhance the power oscillation damping. These relationships provide new insights into the design of the control methods for DGs in microgrid.**

***Index Terms*—Droop control, microgrid, virtual impedance.**

I. Introduction

MICROGRID is a future trend of integrating renewable generation units in a distribution energy system, which consists of various inverter-based distributed generators (DGs). In microgrid, the voltage/frequency stability and accurate load sharing are two important tasks. As three dominated solutions, virtual impedance, angle droop, and frequency droop have been separately developed for over a decade.

Virtual impedance method is early introduced to shape desired output impedances in uninterruptible power systems [1]. Then, it is widely utilized to decouple *P*-*Q* and eliminate reactive-power differences in microgrid due to the line impedance mismatch [2], [3].

Manuscript received July 19, 2016; revised October 22, 2016 and December 29, 2016; accepted January 31, 2017. Date of publication March 2, 2017; date of current version June 9, 2017. This work was supported in part by the National Natural Science Foundation of China under Grant 61622311 and Grant 61573384, and in part by the Project of Innovation-driven Plan in Central South University.

Y. Sun, X. Hou, J. Yang, H. Han, and M. Su are with the School of Information Science and Engineering, Central South University, Changsha 410083, China (e-mail: yaosuncsu@gmail.com; houxc10@csu.edu.cn; jian.yang@csu.edu.cn; hua_han0523@csu.edu.cn; sumeicsu@mail.csu.edu.cn).

J. M. Guerrero is with the Department of Energy Technology, Aalborg University, 9220 Aalborg East, Denmark (e-mail: joz@et.aau.dk).

Color versions of one or more of the figures in this letter are available online at http://ieeexplore.ieee.org.

Digital Object Identifier 10.1109/TIE.2017.2677328

The angle droop control is developed to ensure proper load sharing in a rural distribution network with highly resistive lines [4]. As it directly regulates the converter output voltage angle, a significant steady-state frequency drop is avoided.

The conventional P-ω frequency droop control is firstly proposed to achieve power sharing in parallel inverters without communication [5]. The basic idea of this control manner is to mimic the behavior of synchronous generators [6]. In addition, a larger value of droop gains improves power sharing accuracy, but increases the deviation of frequency/voltage from their normal values, resulting in a tradeoff [7].

Generally, virtual impedance method, angle droop, and frequency droop control are utilized with different purposes in microgrid. But, sometimes they produce similar effects: 1) both virtual impedance and angle droop control are practicable to the highly resistive lines of microgrid; 2) the reactive power sharing can be ameliorated by regulating virtual impedance and Q–V droop gain, respectively.

To explain these phenomena, the analogous relationships among them are discussed in this letter. First, this study provides a new insight to deal with virtual impedance. In fact, virtual inductance can be regarded as a $P-\delta$ and Q–V feedback control, which is similar to an angle droop. Second, after taking the derivative form of angle droop, the equivalent character of virtual inductance is inherently a derivative type $P-\omega$ frequency droop and proportional type Q–V droop control. Third, by combining frequency droop and virtual inductance method, a modified proportional–derivative (PD) type $P-\omega$ frequency droop control is obtained to improve transient stability. With thoroughly discussing these fundamental relationships, this letter gives new perspectives of the unified control law when designing and tuning controllers.

II. Comparing Virtual Impedance With Droop Control

A. Fundamental Concept of Frequency Droop

The conventional frequency droop control is expressed as follows in the inductive wires of ac microgrid [5]:

$$\omega_r = \omega^* - mP,\ \ m \le \frac{\omega_{\max}-\omega_{\min}}{P^*} \tag{1}$$

$$V_r = V^* - nQ,\ \ n \le \frac{V_{\max}-V_{\min}}{Q^*} \tag{2}$$

where ω_r and V_r are the angular frequency and voltage amplitude references of a voltage source inverter (VSI), respectively.

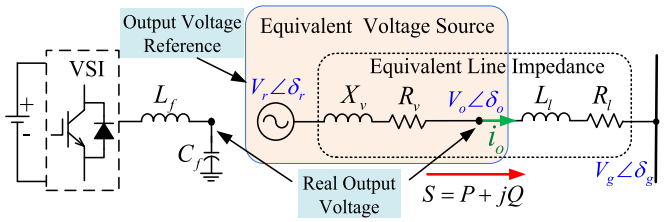

Fig. 1. Equivalent output voltage source considering virtual impedance.

ω^* and V^* represent values of ω and V at no load, and m and n are droop gains of $P-\omega$ and Q–V, respectively. P^* and Q^* are the rated active and reactive power. $\omega_{\max}$ and $\omega_{\min}$ are maximum and minimum values of the allowable angular frequency; and $V_{\max}$ and $V_{\min}$ are maximum and minimum values of the allowable voltage amplitude, respectively.

For a system with a same steady-state operation frequency, the $P-\omega$ droop coefficients of multiple DGs should satisfy the relationship $(m_1P_1^* = m_2P_2^* = \cdots = m_nP_n^*)$ [5]. Thus, it can be ensured that load demands are taken up among DGs in proportion to their power ratings.

B. Equivalence of Virtual Impedance and Angle Droop

The virtual impedance method is used to shape the output impedance of VSI, as shown in Fig. 1. It drops the output voltage reference proportionally to the output current

$$v_o = v_r - Z_v i_o \tag{3}$$

where $Z_v = R_v + jX_v$ is the virtual impedance. $v_o = V_o\angle\delta_o$ and i_o are the output voltage and current, respectively. $v_r = V_r\angle\delta_r$ is the voltage reference of voltage-current dual closed loop.

According to Fig. 1, we have

$$V_o\angle\delta_o\left(\frac{V_r\angle\delta_r - V_o\angle\delta_o}{R_v + jX_v}\right)^* = P + jQ. \tag{4}$$

By substituting output power for output current in (3), power flowing through virtual impedance yields the associated voltage drop ΔV and phase angle difference δ_v. Simplifying (4) yields the following equations:

$$\Delta V = V_r - V_o \cong \frac{R_vP + X_vQ}{V_o} \tag{5}$$

$$\delta_v = \delta_r - \delta_o \cong \frac{X_vP - R_vQ}{V_oV_r} \tag{6}$$

where V_r and δ_r are magnitude and angle of the reference voltage, respectively. V_o and δ_o are magnitude and angle of the output voltage, respectively.

For simplicity, V_r and V_o are replaced by V^* because their voltage magnitudes lie in the acceptable range of the nominal voltage deviation. Moreover, to meet the application condition of conventional droop control, virtual impedance is designed as pure inductance [9]. Then, (7) and (8) are derived from (5) and (6)

$$\delta_o = \delta_r - m_dP \tag{7}$$

$$V_o = V_r - n_dQ \tag{8}$$

where

$$m_d = \frac{X_v}{V^{*2}}\ ;\ n_d = \frac{X_v}{V^*}. \tag{9}$$

From (7) and (8), virtual inductance is regarded as a $P-\delta$ and Q–V feedback control. Especially, (7) is equivalent to angle droop in [4], and (8) is the conventional Q–V droop control. Majumder *et al.* [4] has proved that larger coefficients $m_{\rm d}$ and $n_{\rm d}$ can greatly improve the power sharing. Actually, it means that a larger virtual inductance is adopted to ameliorate line impedance mismatch. This equivalence provides a physical-based insight to tune the parameters of angle droop control.

C. Analogy Between Angle Droop and Frequency Droop

By taking the derivative from the both sides of (7), the equivalent character of virtual inductance is given by

$$\omega_o = \omega_r - m_d\frac{dP}{dt} \tag{10}$$

where ω_r is the angular frequency reference. Usually, a derivative term of active power is replaced by a high-pass filter to suppress interference. Thus, (10) takes the form

$$\omega_o = \omega_r - \frac{m_ds}{s+\omega_c}P \tag{11}$$

where ω_c is the cutoff frequency of the high-pass filter.

From (11), virtual inductance method can be viewed as a special $P-\omega$ frequency droop control, whose droop gain is a washout high-pass filter [8]. In contrast to the static feedback of (1), the washout filter-based active power sharing does not cause the frequency deviation. In addition, it should be noted that the proposed washout filter-based reactive power sharing in [8] cannot improve the reactive power sharing.

D. Improved Droop Control by Combining Virtual Inductance Method and Frequency Droop

Usually, virtual inductance and frequency droop control are simultaneously adopted. Therefore, a modified droop control is presented as follows by substituting (1) and (2) into (8)–(10):

$$\omega_o = \omega^* - mP - m_d\frac{dP}{dt} \tag{12}$$

$$V_o = V^* - (n+n_d)Q. \tag{13}$$

Clearly, the $P-\omega$ droop is changed to a PD type frequency droop control in (12). According to (13), an equivalent Q–V droop gain n_d resulting from virtual inductance, is added to improve the reactive power sharing.

For the power angle dynamics, the PD type control of frequency droop (12) is basically equivalent to the PI type control

TABLE I
ANALOGOUS RELATIONSHIPS AMONG VIRTUAL INDUCTANCE METHOD, ANGLE DROOP, AND FREQUENCY DROOP IN AC MICROGRID

Equivalent feedback control	Advantages		Potential drawbacks
Virtual inductance control (3) Angle droop control (7) Washout filter-based method (11)	✓ Without communication ✓ Constant frequency regulation ✓ Improved power sharing performance ✓ Not affected by the physical parameters	✓ 1 DOF ✓ 2 DOF	✗ Cannot guarantee accuracy power sharing ✗ Require global positioning system (GPS) signals to synchronize DGs ✗ Marginally stable system, poor robustness ✗ Slow dynamic response
Frequency droop+ Virtual inductance (1) + (3) PD type frequency droop (12)	✓ Without communication ✓ Accuracy active power sharing ✓ Satisfactory transient progress ✓ Robust to system parameters	✓ 1 DOF ✓ 2 DOF	✗ Frequency deviation ✗ Require relatively high bandwidth for controller

of phase droop (14), which is more practical to implement without introducing external disturbance

$$\delta_o = \delta^* - m\int_{-\infty}^{t} Pd\tau - m_d P. \tag{14}$$

III. SMALL SIGNAL ANALYSIS

Small-signal analysis of (12) is an effective tool to reflect the power angle response. According to Fig. 1, the output instantaneous active power p of VSI is expressed as [1]

$$p = \frac{V_o V_g}{Z}\cos(\theta - \delta_l) - \frac{V_g^2}{Z}\cos\theta \tag{15}$$

where Z and θ are the magnitude and phase of the output line impedance. $V_g\angle\delta_g$ is the common bus voltage. δ_l is the power angle, expressed as

$$\delta_l = \delta_o - \delta_g. \tag{16}$$

Using the linearized model (15) and (16), the corresponding transient model around the steady-state is formed

$$\Delta p = k_{P\delta}\Delta\delta_l;\ \Delta\delta_l = \Delta\delta_o - \Delta\delta_g = \frac{1}{s}(\Delta\omega_o - \Delta\omega_g) \tag{17}$$

where $k_{P\delta} = \partial p/\partial\delta_l$ is a differential coefficient.

In the small signal modeling, the low-pass power filter is usually added to obtain the average active power and avoid the external disturbance from the power derivation [10], [11]. The output characteristic of modified droop in (12) is given by

$$\Delta\omega_o = \Delta\omega^* - \frac{m + m_d s}{\tau s + 1}\Delta p. \tag{18}$$

Substituting (18) in (17) yields

$$\Delta p = \frac{(\tau s + 1)k_{P\delta}}{\tau s^2 + (1 + m_d k_{P\delta})s + m k_{P\delta}}(\Delta\omega^* - \Delta\omega_g). \tag{19}$$

For a typical second-order model of characteristic equation in (19), the damping ratio ζ is obtained in (20) and usually chosen between 0.4 and 0.8 [12]

$$0.4 \le \zeta = \frac{1 + m_d k_{P\delta}}{2\sqrt{m k_{P\delta}\tau}} \le 0.8. \tag{20}$$

By tuning parameters, τ and m_d, the transient response can be regulated appropriately without compromising steady state. The function of a derivative feedback is to enhance dynamic stability.

To design the droop gains $(m,\ n,\ m_d,\ n_d)$ properly, the issues such as proportional power sharing, voltage quality, and stability should be considered.

1) When choosing the proportional $P-\omega$ droop coefficient m, the real power sharing is guaranteed among DGs according to their power ratings [5]. Meanwhile, the frequency deviation in (1) should be limited in a feasible range.
2) The coefficient m_d should be designed according to (20) for a better dynamic response.
3) The coefficients n and $n_{\rm d}$ have a same effect on improving reactive power sharing. But, there is a tradeoff between the reactive power accuracy and the voltage deviation [7]. The voltage deviation in (2) should be limited in the feasible range.
4) At last, the designed droop gains must guarantee stability. For more details, please refer to references [10], [13].

Furthermore, as virtual inductance only provides one degree of freedom (DOF) in (9), m_d and n_d are dependent. Therefore, transient response and reactive power sharing cannot be separately regulated by virtual inductance. Alternatively, the modified droop control in (12) and (13) should be adopted. On the whole, the analogous relationships among these control strategies are presented in Table I.

IV. SIMULATION RESULTS

To verify the unified control law between the conventional droop control with virtual inductance and the modified droop control (12), (13), the control scheme and simulation model with three parallel-connected DGs are built in Fig. 2. The reference voltage at no load is 220 V/50 Hz.

First, the frequency droop control (1), (2) with gains $m = 3\times10^{-4}$ and $n = 1\times10^{-3}$ is tested. As shown in Fig. 3(a.1)–(d.1), the dynamic responses of the power have several cyclical oscillations and the system arrives to the steady state within a second. In addition, the accuracy of reactive power sharing is low due to the mismatch of the line impedance.

Second, to overcome the drawbacks of conventional frequency droop control, a virtual reactance of $0.9\,\Omega$ is added in Fig. 2. From simulation results in Fig. 3(a.2)–(d.2), the active power has a fast and good response during load change. And the accuracy of reactive power sharing is acceptable.

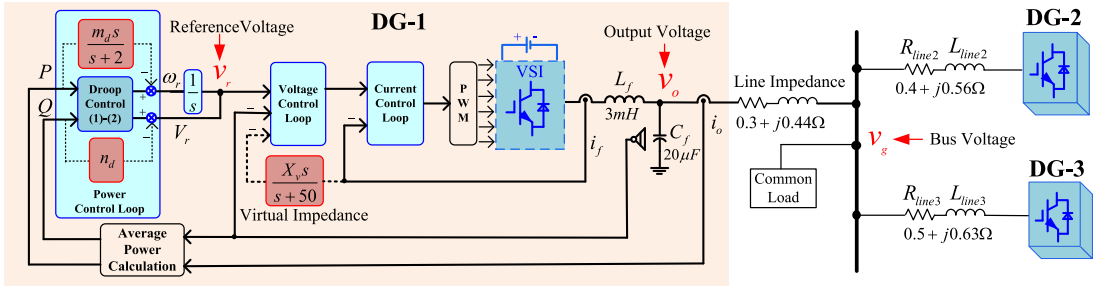

Fig. 2. Control schematic and test model of simulations in MATLAB/simulink.

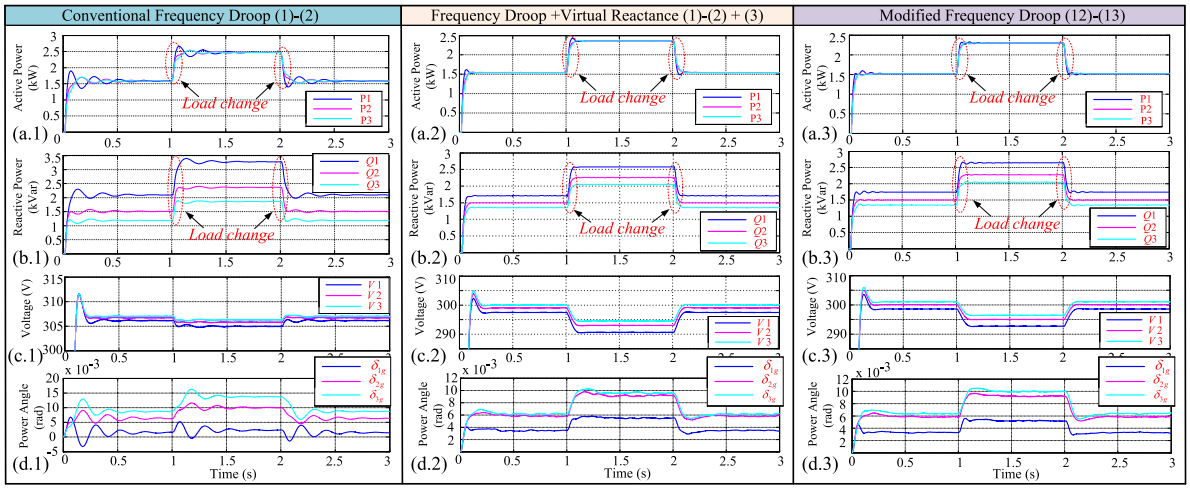

Fig. 3. Comparisons of (a) active power, (b) reactive power, (c) voltage amplitude, and (d) power angle under three methods.

TABLE II
EXPERIMENT PARAMETERS

Voltage reference	$f^* = 50$ Hz, $V^* = 48$ V
Line parameters	$Z_1 = 0.1 + j0.18\ \Omega$, $Z_2 = 0.1 + j0.47\ \Omega$
Virtual reactance	$X_v = 1.5\ \Omega$
Frequency droop	$m = 4 \times 10^{-3}$, $n = 1 \times 10^{-2}$
Modified droop	$m_d = 6 \times 10^{-4}$, $n_d = 3 \times 10^{-2}$
Load 1/ Load 2	$Z_{L1} = 20 + j3.14\ \Omega$, $Z_{L2} = 10 + j2.51\ \Omega$

Finally, the modified droop control (12) and (13) is adopted to verify the inherent analogy with virtual inductance method. According to (9), $m_d = 1 \times 10^{-5}$ and $n_d = 3 \times 10^{-3}$. Fig. 3(a.3)–(d.3) reveal that the modified droop (12) and (13) have the equivalent functions to the frequency droop plus virtual inductance. Compared with the second case of virtual inductance, m_d and n_d are dependent, and the system transient response of and reactive power sharing can be regulated, respectively.

V. EXPERIMENT RESULTS

To verify the advantages of the modified method (12), a microgrid prototype is built based on two single-phase inverters. The experiment parameters are listed in Table II. Similar to the simulations, the frequency droop control (1) and (2), the virtual inductance method (3) and the modified droop method (12) and (13) are compared with experiments. During the initial stage, only load 1 is connected to the common bus. To show the transient response, load 2 is added after a while.

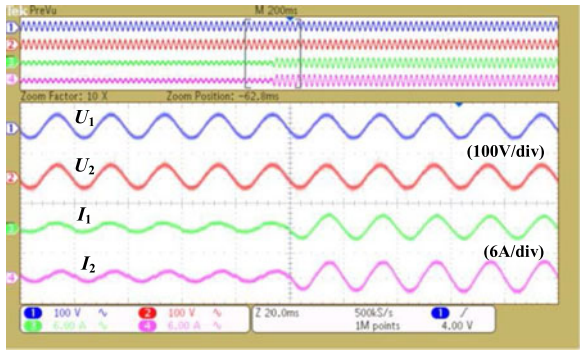

Fig. 4. Voltage/current waveforms in conventional frequency droop (1) and (2).

Fig. 4 shows the measured voltage and current waveforms under the frequency droop control (1), (2). The waveforms from top to bottom are the output voltage $(\boldsymbol{U}_1)$ of inverter 1, the output voltage $(\boldsymbol{U}_2)$ of inverter 2, the output current $(\boldsymbol{I}_1)$ of inverter 1, and the output current $(\boldsymbol{I}_2)$ of inverter 2, respectively. The calculated output active and reactive powers are illustrated in Fig. 5. As seen, an obvious power oscillation occurs during load change and there is a large reactive power sharing error.

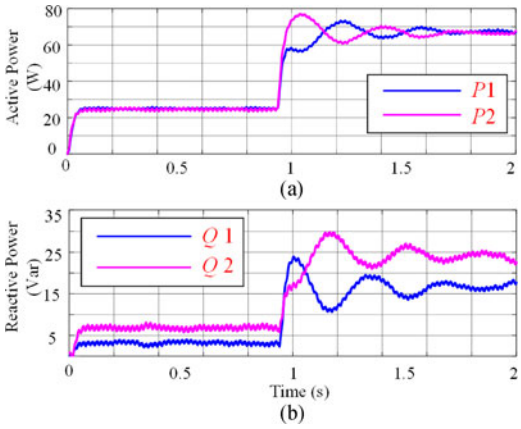

Fig. 5. Power response during load change in conventional frequency droop. (a) Active power and (b) reactive power.

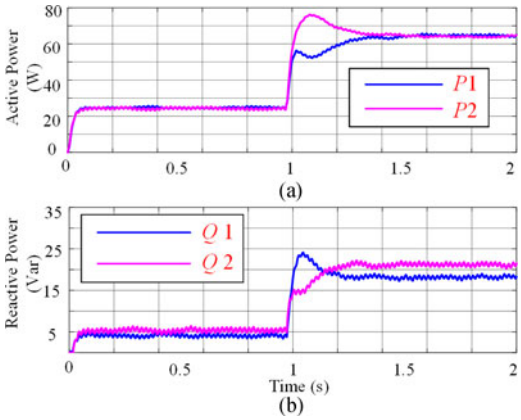

Fig. 6. Power response during load change in frequency droop plus virtual reactance. (a) Active power and (b) reactive power.

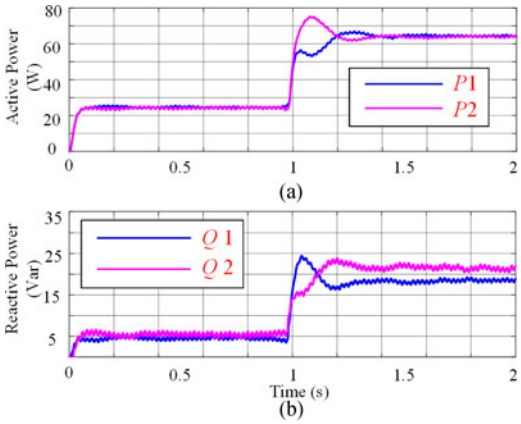

Fig. 7. Power response during load change in modified frequency droop. (a) Active power and (b) reactive power.

To investigate the effects of virtual reactance, the frequency droop with virtual reactance is implemented. The experiment results are shown in Fig. 6. Compared with Fig. 5, Fig. 6 reveals that power oscillation has been well suppressed. And the power sharing accuracy has been improved significantly.

To verify the similarity between the virtual inductance method (3) and the modified droop control (12) and (13), m_d and n_d are carried out according to the deduced equation (9). Fig. 7(a) reveals that the power derivative feedback could effectively increase the power oscillation damping without reducing power sharing accuracy. Fig. 7(b) shows that the added droop gain n_d obtains the same reactive power sharing accuracy as the virtual reactance method of Fig. 6(b).

VI. Conclusion

This letter compared the similarities and differences among three different concepts, virtual impedance method, angle droop, and frequency droop control. Although each of them has been well researched, new perspectives are bought to readers by relating all three together. Thus, the inherent relationships are established, and new insights into the controller design are provided. Finally, the modified droop control unifies these three independently developed droop control methods into a generalized theoretical framework. To the reader, this letter explored the possibilities of further enhancing the existing methods and inspiring the development of new methods.

References

[1] J. M. Guerrero, L. GarciadeVicuna, and J. Matas, "Output impedance design of parallel-connected UPS inverters with wireless load-sharing control," *IEEE Trans. Ind. Electron.*, vol. 52, no. 4, pp. 1126–1135, Aug. 2005.

[2] J. He and Y. Li, "Analysis, design, and implementation of virtual impedance for power electronics interfaced distributed generation," *IEEE Trans. Ind. Appl.*, vol. 47, no. 6, pp. 2525–2538, Nov./Dec. 2011.

[3] H. Mahmood, D. Michaelson, and J. Jiang, "Accurate reactive power sharing in an islanded microgrid using adaptive virtual impedances," *IEEE Trans. Power Electron.*, vol. 30, no. 3, pp. 1605–1617, Mar. 2015.

[4] R. Majumder, G. Ledwich, A. Ghosh, S. Chakrabarti, and F. Zare, "Droop control of converter-interfaced microsources in rural distributed generation," *IEEE Trans. Power Del.*, vol. 25, no. 4, pp. 2768–2778, Oct. 2010.

[5] M. C. Chandorkar, D. M. Divan, and R. Adapa, "Control of parallel connected inverters in standalone ac supply systems," *IEEE Trans. Ind. Appl.*, vol. 29, no. 1 pp. 136–143, Jan. 1993.

[6] S. D'Arco and J. A. Suul, "Equivalence of virtual synchronous machines and frequency-droops for converter-based microgrids," *IEEE Trans. Smart Grid*, vol. 5, no. 1, pp. 394–395, Jan. 2014.

[7] J. M. Guerrero, J. C. Vasquez, J. Matas, L. G. De Vicuna, and M. Castilla, "Hierarchical control of droop-controlled AC and DC microgrids—A general approach toward standardization," *IEEE Trans. Ind. Electron.*, vol. 58, no. 1, pp. 158–172, Jan. 2011.

[8] M. Yazdanian and A. Mehrizi-Sani, "Washout filter-based power sharing," *IEEE Trans. Smart Grid*, vol. 7, no. 2, pp. 967–968, Mar. 2016.

[9] C. Li, S. K. Chaudhary, M. Savaghebi, J. C. Vasquez, and J. M. Guerrero, " Power flow analysis for low-voltage AC and DC microgrids considering droop control and virtual impedance," *IEEE Trans. Smart Grid*, to be published.

[10] E. A. A. Coelho, P. C. Cortizo, and P. F. D. Garcia, "Small signal stability for parallel-connected inverters in stand-alone AC supply systems," *IEEE Trans. Ind. Appl.*, vol. 38, no. 2, pp. 533–542, Mar. 2002.

[11] E. A. A. Coelho *et al.*, "Small-signal analysis of the microgrid secondary control considering a communication time delay," *IEEE Trans. Ind. Electron.*, vol. 63, no. 10, pp. 6257–6269, Oct. 2016.

[12] K. Ogata, *Modern Control Engineering*. Englewood Cliffs, NJ, USA: Prentice-Hall, 2001, pp. 170–171.

[13] G. Diaz, C. Gonzalez-Moran, J. Gomez-Aleixandre, and A. Diez, "Scheduling of droop coefficients for frequency and voltage regulation in isolated microgrids," *IEEE Trans. Power Syst.*, vol. 25, no. 1, pp. 489–496, Feb. 2010.